HAL
open science

Dynamic model of a PAD actuator : dynamic operations and pull-off at high speed

Christophe C. Giraud-Audine, Michel Amberg, Frédéric Giraud, Charles Mangeot, Betty Lemaire–semail

To cite this version:

Christophe C. Giraud-Audine, Michel Amberg, Frédéric Giraud, Charles Mangeot, Betty Lemaire–semail. Dynamic model of a PAD actuator : dynamic operations and pull-off at high speed. ACTUATOR 2016, Jun 2016, BREMEN, Germany. hal-01427184

HAL Id: hal-01427184

https://hal.science/hal-01427184v1

Submitted on 5 Jan 2017

HAL is a multi-disciplinary open access archive for the deposit and dissemination of scientific research documents, whether they are published or not. The documents may come from teaching and research institutions in France or abroad, or from public or private research centers.

L'archive ouverte pluridisciplinaire **HAL**, est destinée au dépôt et à la diffusion de documents scientifiques de niveau recherche, publiés ou non, émanant des établissements d'enseignement et de recherche français ou étrangers, des laboratoires publics ou privés.

Dynamic model of a PAD actuator : dynamic operations and pull-off at high speed

Christophe GIRAUD-AUDINE* 1 , Michel AMBERG 1 ,Frédéric GIRAUD 1 , Charles MANGEOT 2 , Betty LEMAIRE−SEMAIL 1
1 Univ. Lille, Centrale Lille, Arts et Metiers ParisTech, HEI, EA 2697 - L2EP - Laboratoire d'Electrotechnique et d'Electronique de Puissance, F-59000 Lille, France
2 NOLIAC A/S, Hejreskovvej 18,3490 Kvistgaard, Denmark

Abstract: The PAD motor has remarkable abilities for ultra-precise positioning at very low speed. Recent works have shown the possibility to extend its speed range, but some challengess remain such as pull-off. This paper proposes a model that highlights the parameters of the voltage supply that act on the torque and the contact, and can be used for control. Experimental results demonstrate the role of higher vibration modes, and show that typical signature of the imminence of pull-off can be detected thanks to some of the harmonic of the displacement of the actuators, giving some indications on means to address this problem.

Keywords: PAD motor, pull-off, dynamic model

1-Introduction

PAD motors are low speed, precision motors manufactured by NOLIAC. Initially, the operations being slow, this type of motor can be considered as quasi-static motors. Recent studies have shown that the PAD could be driven at higher speed up to and beyond resonance. However, in [1] some difficulties were observed in the vicinity of resonance due the relative phase of the vibration resulting from the sudden phase rotation near the resonant frequencies of the actuators.

This paper proposes a simplified model of the PAD dynamics including the contact to address this issue. It provides some insight in the phenomena affecting the contact forces and the torque, and can describe the dynamic at higher frequencies. Furthermore, an experimental study shows that the motor can operate at frequencies higher than the free resonant frequencies of the actuators. Besides, the results indicate that the pull off resulting in the stalling of the motor is not only due the voltages applied but also to vibratory behaviour at the contact.

In the first part, the dynamic model is explained. The pull-out and the torque generation mechanism is explained in quasi static operation, and the dynamic equations are modified to yield a simplified model. In the second part, some experiments are presented. Using a frequency analysis, some insight of the vibratory behaviour of the actuators is gained, and a typical signature of the imminence of stalling is identified.

2-Theoretical study

Equilibrium of the crowned wheel

The PAD motor features two sets of actuators acting along two perpendicular directions, so as to generate a circular translation applied to a crown wheel (Fig. 1, top). When brought into contact with a geared shaft, this wobbling movement is converted into a rotation of the shaft. The micro gear adds a high gear ratio thus allowing ultra low speed operation and exceptional positioning capabilities. To obtain the wobbling, the actuators are driven using two sinusoidal voltages shifted by 90°.

On the same figure, the motor is depicted during operation. Voltages are applied to the actuators, inducing their deformations. The forces applied to the crown wheel are given by :

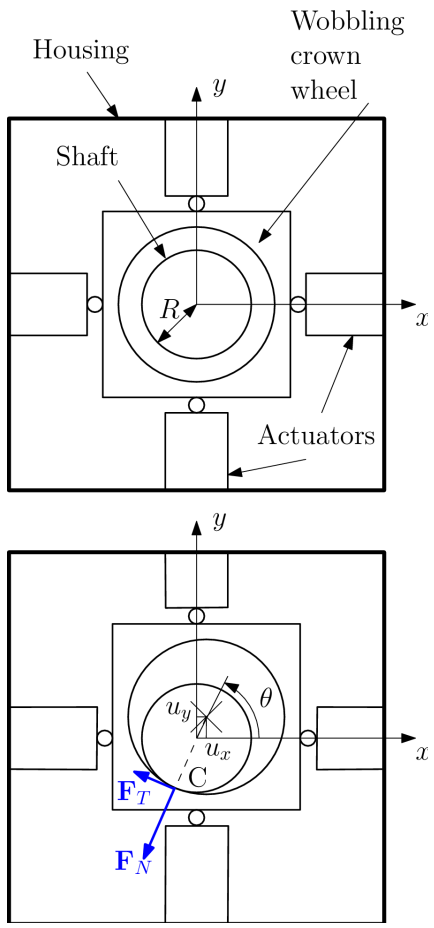

Figure 1 : schematic of the structure of the Pad motor (up) and during operation (bottom)

$$F_a = 2\begin{pmatrix} N V_x - K_s u_x \\ N V_y - K_s u_y \end{pmatrix} \quad (1)$$

where N and K_s are the piezoelectric actuator force factor and rigidity respectively. u_x, u_y, V_x and V_y are the displacement of the piezoelectric actuator tips and the voltages applied for the x and y direction respectively.
The normal force at the contact point C is modelled as an elastic contact (rigidity k) such that :

$$F_N = -k\left(1-\frac{R}{d}\right)\begin{pmatrix} u_x \\ u_y \end{pmatrix} \quad (2)$$

where $d=\sqrt{u_x^2+u_y^2}$ and R is the radius of the shaft.
Finally, the tangential force at the contact point can be related to the torque T applied by the crowned wheel on the shaft by:

$$F_T = \frac{T}{R}\begin{pmatrix} -\sin\theta \\ \cos\theta \end{pmatrix} \quad (3)$$

where θ is the direction of the displacement vector.
It should be noted that the simplified contact model supposes that d>R that is, strictly speaking, that the crowned wheel intersect the shaft. However, k being large the error can be considered to be small, and moreover, R represent the addendum circle of the shaft.
To obtain the dynamic model, in contact condition, one writes Newton's first law applied to the crowned wheel yielding:

$$\begin{aligned} -(2K_s+k)u_x + kR\cos\theta - \frac{T}{R}\sin\theta + 2NV_x = M\ddot{u}_x \\ -(2K_s+k)u_y + kR\sin\theta - \frac{T}{R}\cos\theta + 2NV_y = M\ddot{u}_y \end{aligned} \quad (4)$$

The equation above can be extended to the non contact operations by letting k=0 and cancelling T.

Static characteristics

Cancelling the accelerations in the previous equations and replacing $u_x = d\cos\theta$ and $u_y = d\sin\theta$, one can get the following static equations thanks to trigonometrical identities :

$$\begin{aligned} -(2K_s+k)d + kR + 2N(V_u\cos\theta + V_y\sin\theta) = 0 \\ \frac{T}{R} = 2N(V_u\sin\theta - V_y\cos\theta) \end{aligned} \quad (5)$$

Since the voltages applied are two phase in quadrature, we write $V_x = V\cos\phi$ and $V_y = V\sin\phi$ and finally the torque can be rewritten as:

$$T = 2NRV\sin(\theta-\phi) \quad (6)$$

and the displacement of the crowned gear is:

$$d = \frac{kR + 2NV\cos(\theta-\phi)}{2K_s+k} \quad (7)$$

These equations show that the static performances are driven by :

1. the amplitude of the voltage
2. the "phase shift" between the actual position of the crowned gear and the voltages phase

It is possible to derive some conditions. First the contact must exist as a premise to the operations, that is $R=d$ defines a limit. Thus, replacing this condition in (7), and expressing the sine of the phase shift as a function of the applied torque and voltage amplitude, the limit equation is:

$$V = \frac{1}{2N}\sqrt{(2K_sR)^2 + \left(\frac{T}{R}\right)^2} \quad (8)$$

together with the limit phase shift:

$$\theta - \phi = \arctan\frac{T}{2K_sR^2} \quad (9)$$

Actually, (8) and (9) represent limit cases, and thus the actual feasible regions are depicted on Figure 2 and 3 using normalized values for the sake of generality. The voltage amplitude should be in the area enclosed at the intersection of the voltage greater than the limit given by (8) and below the maximum voltage of the piezoelectric actuators. The corners of this area are the maximum realizable torque (note however that on the figure the indicated values are only indicative and not related to the actual actuator).

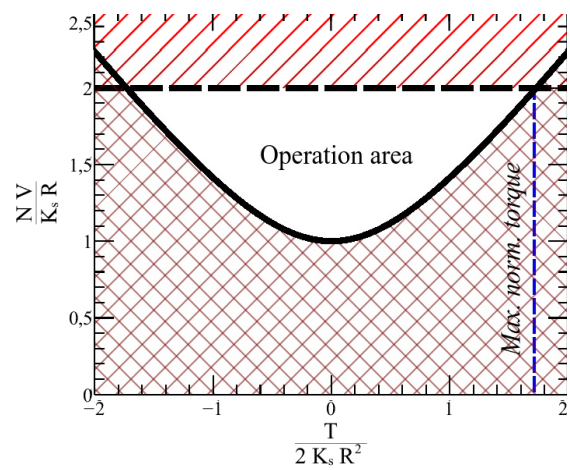

Figure 2 : Theoretical operating area of the model of the PAD motor

Figure 3 shows that the phase shift should be greater than the limit given by (9). On the graph the limit due to voltage limitation is also represented and, again, is only indicative. An interesting point on this figure is that it becomes clear that the phase shift will control motor or braking operations.

Dynamic model

To describe the dynamic of the shaft, the following equation has to be added to equations (4):

$$J\ddot{\psi} = T_m - T_l \quad (10)$$

where ψ is the shaft angle, J is the shaft inertia, T_m and T_l are the motor and load torque respectively. Due to the gearing, the crowned wheel angle and the shaft angle are linked by the following relationship if the contact is ensured: $\psi = \gamma\theta$ (11)
where γ is the reduction ratio of the gearing. Therefore , the following relation between the torques holds: $T = \gamma T_m$.

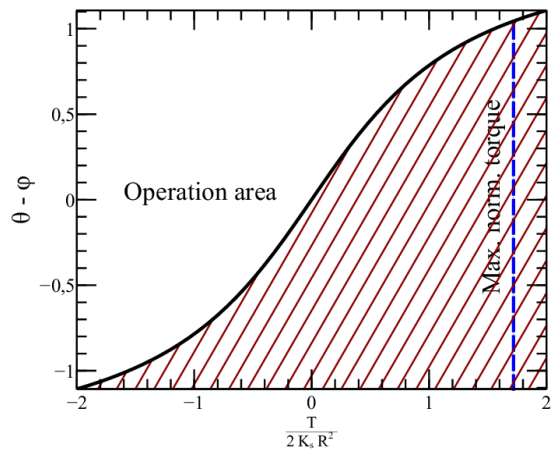

Figure 3 : Theoretical phase shift vs normalized torque and corresponding operation area

Figure 4 depict the diagram of the dynamic equilibrium of the crowned wheel in sinusoidal steady state i.e. $\boldsymbol{u}=\hat{\boldsymbol{u}}e^{i\omega t}$. In this case, the inertial force will be $-M\ddot{\boldsymbol{u}}=M\omega^2\boldsymbol{u}$ where ω is the angular frequency of the voltages and, since synchronism is imposed by the gearing, the rotor speed i.e. $\dot{\theta}=\omega$. From this diagram, it can be deduced that as the speed increases, the forces applied by the actuators F_{ax} and F_{ay} should be increased to maintain the normal and tangential forces F_N and F_T respectively.

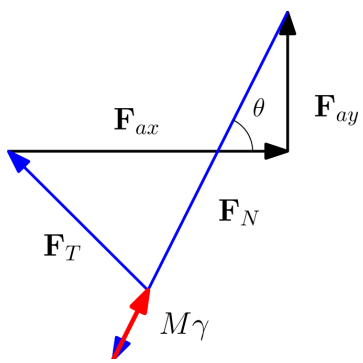

Figure 4 : vector diagram of the dynamic equilibrium of the crowned wheel.

In order to do so, the voltages amplitude should be increased. In other words, as the speed increases, assuming constant voltages, and provided that to maintain the contact a limit normal force is required, the motor will be more prone to "pull off" that is the transmission between the gear will be lost. In order to estimate this, a more elaborated model of the contact should be developed. In the following, an experimental study is presented to estimate the occurrence of pull off in the case of the motor under investigation.

Experimental set up

The experiment was designed to investigate the dynamical behaviour of the motor, with a special emphasis on the pull off. It was therefore necessary to have a measurement of the actual displacement of the actuator. In the model at hand, the actuators are piezoelectric multilayer benders. In these actuators the outermost layer is usually not electroded to provide some isolation. The PAD motor actuators were modified by creating an additional electrode (Fig. 5). As deformation occurs, due to the direct piezoelectric effect, a voltage will be induced which is proportional to the difference of slopes at the end of the electrode [3] . Therefore, for a given mode, the measured voltage is proportional to the amplitude of the vibration.

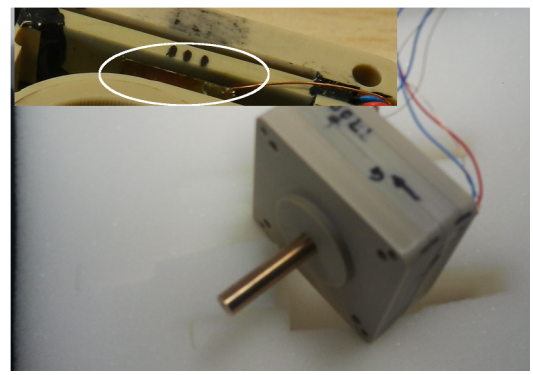

Figure 5 : Picture of the PAD motor and detail of one of the implemented sensor electrodes (upper left side)

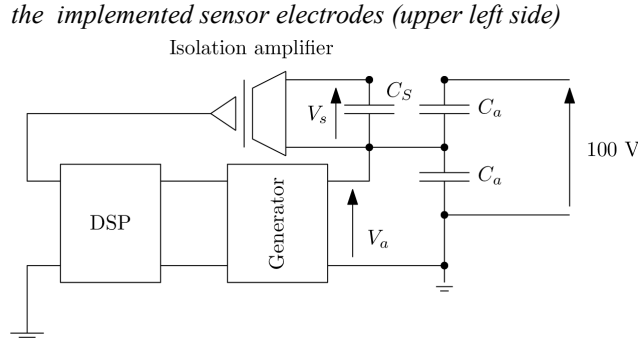

Figure 6 : Schematic of the sensor implementation

On Fig. 6, the electrical circuit of the set up is depicted. The capacitances C_a represent the capacitance of a section of an actuator. The bender must be polarized to 100 V, and the motion is obtained by imposing the voltage V_a. Due to the internal structure of the actuators, the last layer used for the sensor (represented by the capacitance C_s) is connected to V_a. A floating measurement using an isolation amplifier is thus necessary. The voltages delivered by the sensing piezoelectric layer can vary up to 60 V, hence, it was preferred to measure the current through a shunt resistor on the high voltage side, that is the motional current rather than the voltage V_s was measured.

On Fig . 7, the measurement of the motional current vs frequency is presented for the motor without the shaft. The resonances of the first mode are correctly detected, and the cross talk between the two axes is small. It can be

noted that the resonant frequencies are 20 Hz apart as mentioned in [1], which may cause the problem described in the introduction.

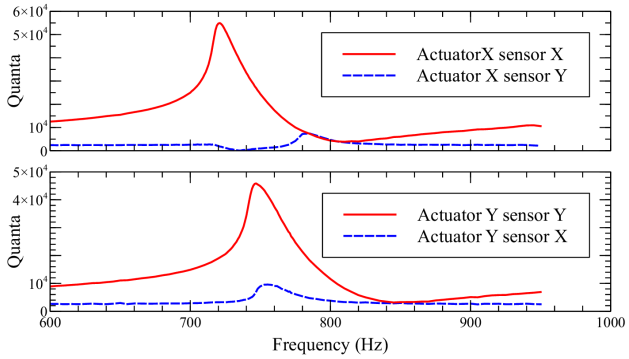

Figure 7 : Measurement vs frequency of the motional current sensors

Experimental results

As represented on Fig. 6, the sensors signals were processed thanks to a DSP. A DFT algorithm synchronised on the supply voltages was then implemented to analyse the dynamical behaviour. The tests consist in varying the frequency at the end of each period thus approaching a sweep signal, so the speed is varying linearly.

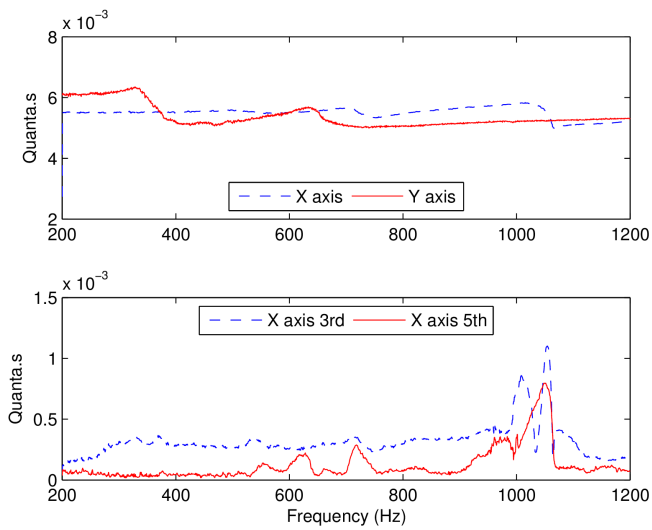

Figure 8: Frequency response of the displacement with mounted shaft for small amplitude radial vibrations

The first experiment consists in reiterating the frequency response once the shaft is mounted back. The actuators were polarized to ensure contact at θ=0°, and to this DC voltage a sinusoidal voltage was superimposed at 10% of the rated voltage. Hence no rotation occurs, but a small amplitude vibration is generated. The frequency response is modified (Fig. 8) and is very different for each axis. Examining the 3rd and 5th harmonics for axis X, it can be observed that their amplitude tend to increase as the fundamentals amplitude of axis X and Y vary in the vicinity of 380 Hz, 620 Hz, 710 Hz and most dramatically near 1000 Hz. This indicates that the vibration regime changes and possibly shocks occur. It should be noted though that the amplitude varies by a small amount so it can hardly be considered as resonances.

A similar test was conducted at θ=135°, the same kind of vibration were applied, radially as before but also tangentially. Indeed the radial cross section of the crowned wheel is not constant as suggested by Fig. 1, and it can be expected that the small signal behaviour might be dependent on the combined rigidities of the shaft and the crowned wheel.

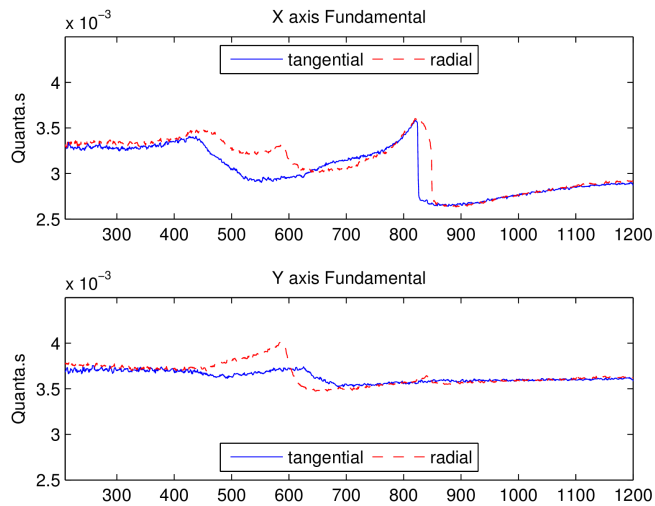

Figure 9: frequency responses of the two axis for small amplitude vibration along the radial and tangential directions

The position of the contact does not have real effect (Fig. 9), but the direction of the vibration does modify the response in the case of the X axis. As a matter of fact, an amplitude jump is clearly visible which can be attributed to intermittent contact of the teeth. Indeed such jumps are typical of oscillators with change of elasticity dependent on the amplitude [3]. To conclude with these low amplitude tests, the motor was supplied by two low amplitude voltages in quadrature, thus inducing the circular translation of the crowned wheel. The frequency response (Fig. 10) exhibits several resonances. Since several mode shapes are excited and the sensitivity of the sensors are dependent on the slope of the shapes at the electrodes, the amplitudes should be considered carefully. Indeed, the sensor electrodes are not identical on each actuator. Hence, although the signals may appear to be larger in some frequency bandwidth, this could also be due to discrepancies of the sensors sensitivity to the different modes excited. The third harmonic is also excited near 1 kHz, and might cause the contact conditions to be degraded. In order to assess the possibility to achieve high speed positioning, the motor was supplied in working conditions at various amplitudes. Pull-off was observed at various frequencies, near 400 Hz

and 1000 Hz depending on the amplitude of the voltage applied.

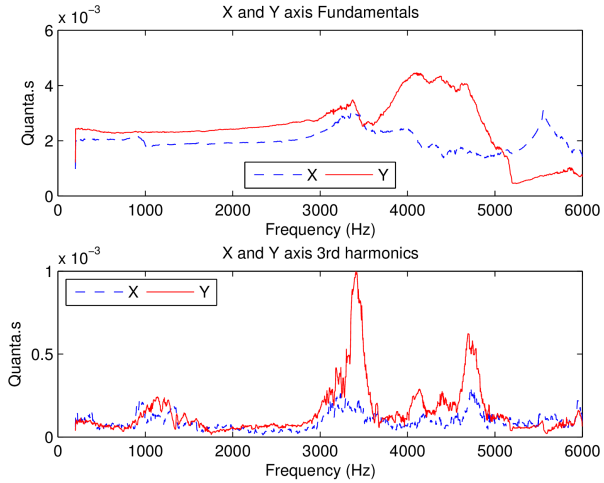

Figure 10: wide band frequency response of displacements for small vibration in circular translation motion

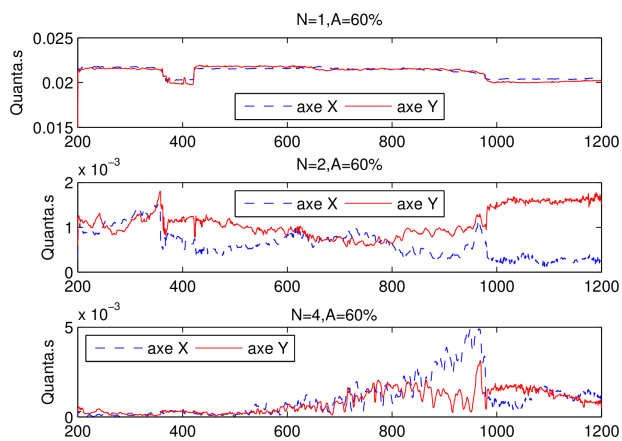

Figure 11: test at 60% of the maximum rated voltage

Some of the results are presented on fig. 11 and 12 for voltage at 60% and 85% of the maximum rated voltages. On Fig.11 the pull-off can clearly be seen at the sudden change in amplitude of the fundamental. Interestingly enough, it can be observed that the motor stops before 360 Hz then starts again at 420 Hz. Finally at 970 Hz, control is completely lost. The most striking feature of this test is the progressive growth of the 2nd and 4th harmonics, before they suddenly collapse when the pull-off occurs. For larger voltages, the pull-off only occurs at 980 Hz which is about 30% higher than the resonance of the motor without shaft. The same trend can be observed on the 4th harmonic.

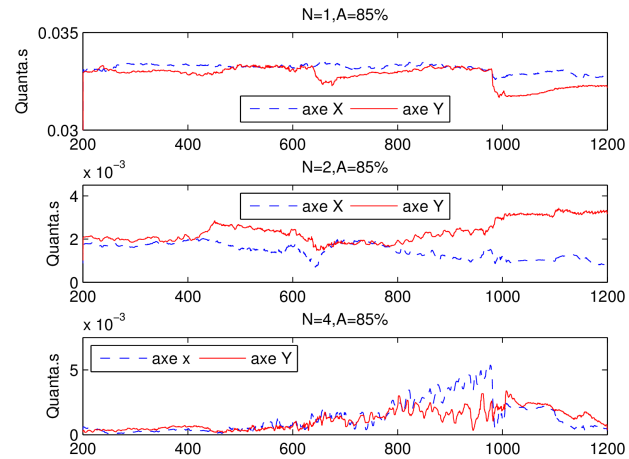

Figure 12: test at 85% of the maximum rated voltage

Discussion and conclusion

This paper has proposed a dynamic model to describe the operation of the PAD actuator and points out the role of the voltage and the phase shift between voltage and contact position. An experimental study was presented to understand the issues that can trigger pull-off. Thanks to the insight offered by a DFT analysis, it has been demonstrated that higher modes, excited by harmonics induced by the contact, could cause the pull off. Moreover, the pull-off is preceded by a variation of the 2nd and 4th harmonics which provides a way to anticipate it. Therefore, future work will extend the model for control purposes. A special attention will be paid to the damping of higher modes. This could be realized by techniques such as the one proposed in [4].

Acknowledgements

This work has been carried out within the framework of the project StimTac of IRCICA (institut de recherche sur les composants logiciels et matériel pour la communication avancée), and the Project Mint of Inria.

References

[1] C. Mangeot, « Operation of a quasi-static piezomotor in transitory frequency range up to resonance », ACTUATOR proceedings 2014.

[2] A. Erturk , D. J. Inman, « An experimentally validated bimorph cantilever model for piezoelectric energy harvesting from base excitations », *Smart Materials and Structures*, vol. 18, n° 2, p. 025009, févr. 2009.

[3] N. Bogolioubov, I. Mitropolski, Méthodes asymptotiques en théorie des oscillations non linéaires, Gauthier-Villars, Paris 1962. (in french)

[4] M. W. Fairbairn, S. O. R. Moheimani, et A. J. Fleming, « Q Control of an Atomic Force Microscope Microcantilever: A Sensorless Approach », *Journal of Microelectromechanical Systems*, vol. 20, n° 6, p. 1372-1381, déc. 2011.